Role of 2,3-bis(pyridyl)pyrazinyl chelate bridging ligand on the reactivity of Ru(II)-Pt(II) dinuclear complexes on the substitution of chlorides by thiourea nucleophiles – kinetic study

Rajesh Bellam*[a], Deogratius Jaganyi*[b], Allen Mambanda and Ross Robinson
[a] School of Chemistry and Physics, University of KwaZulu-Natal, Private Bag X01, Scottsville, Pietermaritzburg 3209, South Africa. [b] College of Science, University of Rwanda, P.O. Box 4285, Kigali, Rwanda.

ELECTRONIC SUPPLEMENTARY INFORMATION (ESI)

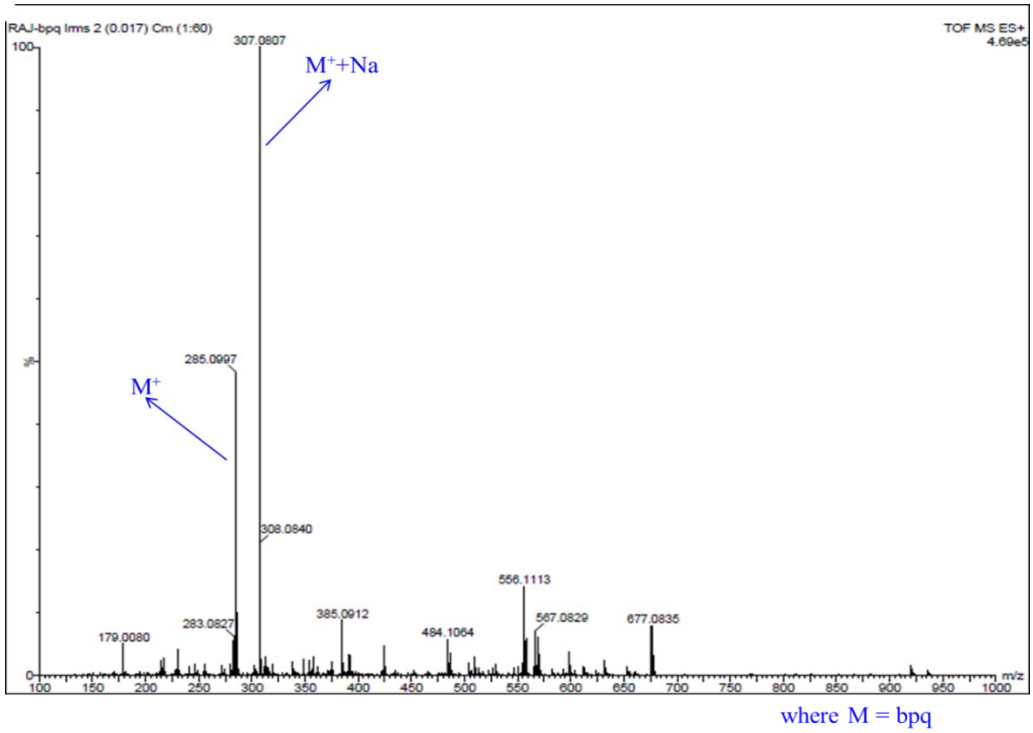

Figure 1 TOF-MS spectra of 2,3-bis(2'pyriyl)-quinoxaline (bpq).

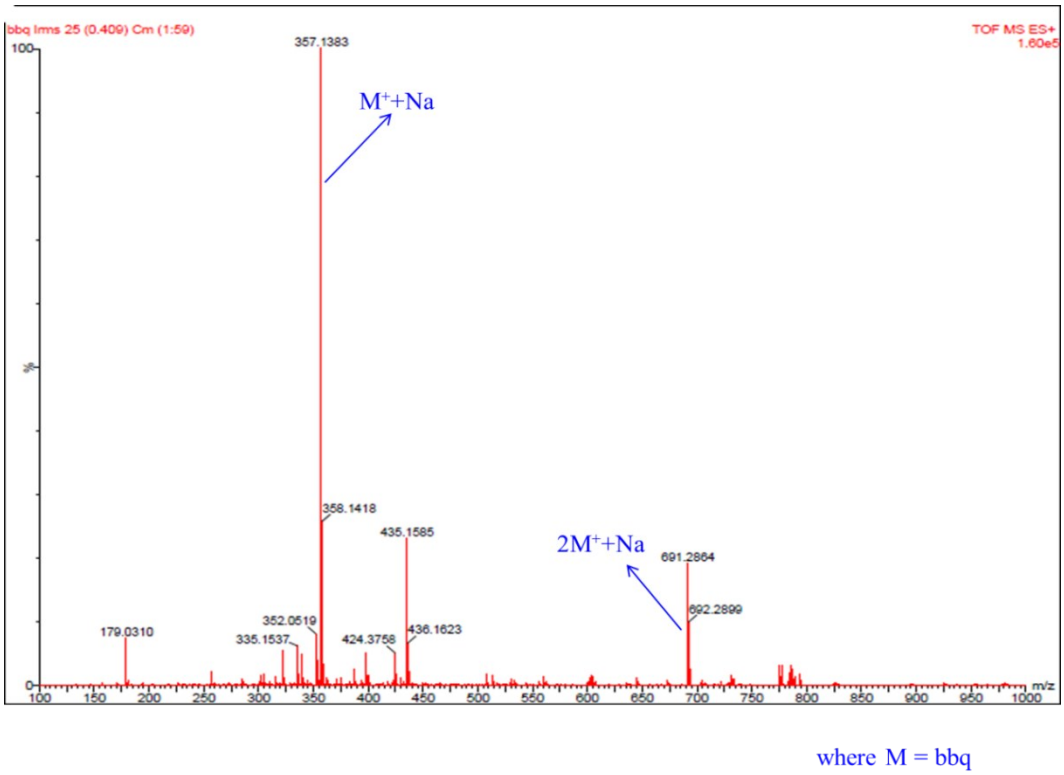

Figure 2 TOF-MS spectra of 2,3-bis(2'pyriyl)benzo[g]quinoxaline (bbq).

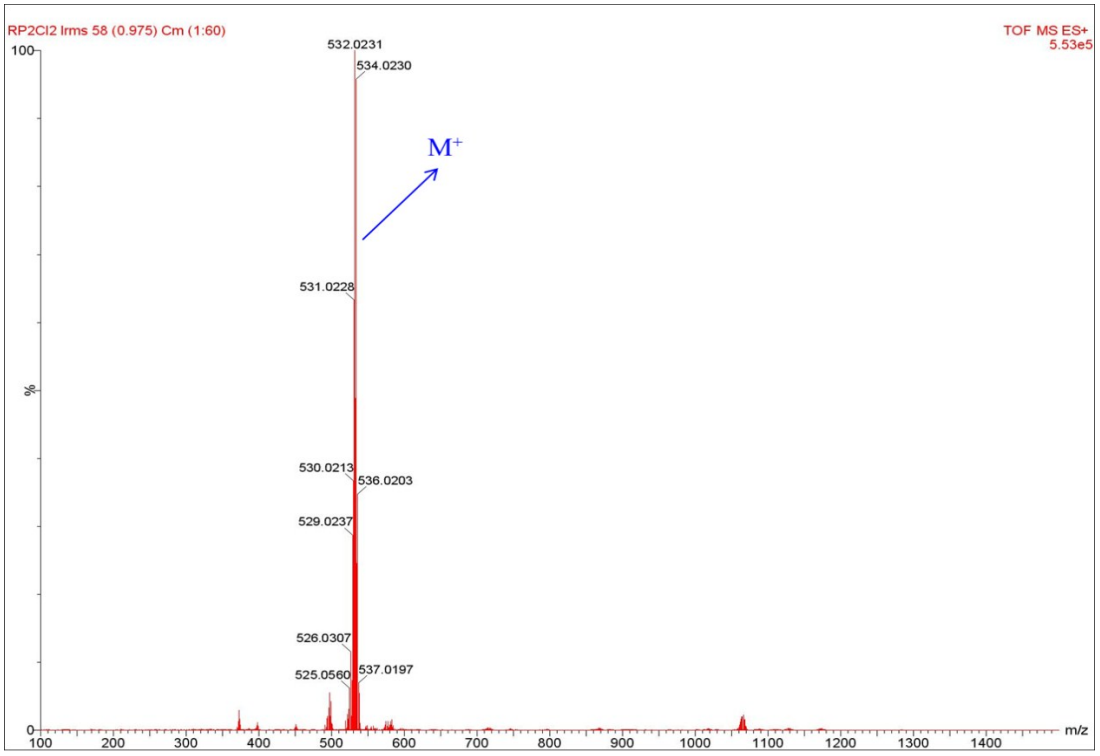

where M = $(Phen)_2RuCl_2$

Figure 3 TOF-MS spectra of $(phen)_2RuCl_2$.

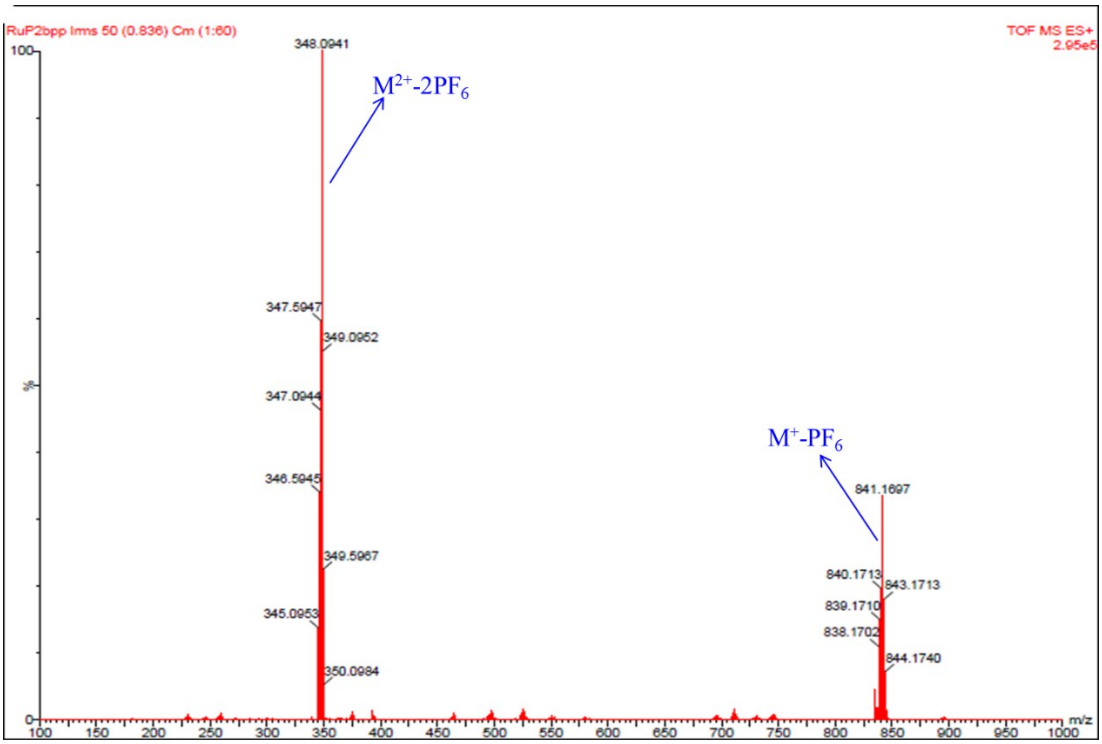

where M = $[(phen)_2Ru(bpp)](PF_6)_2$

Figure 4 TOF-MS spectra of $[(phen)_2Ru(\mu\text{-}bpp)](PF_6)_2$.

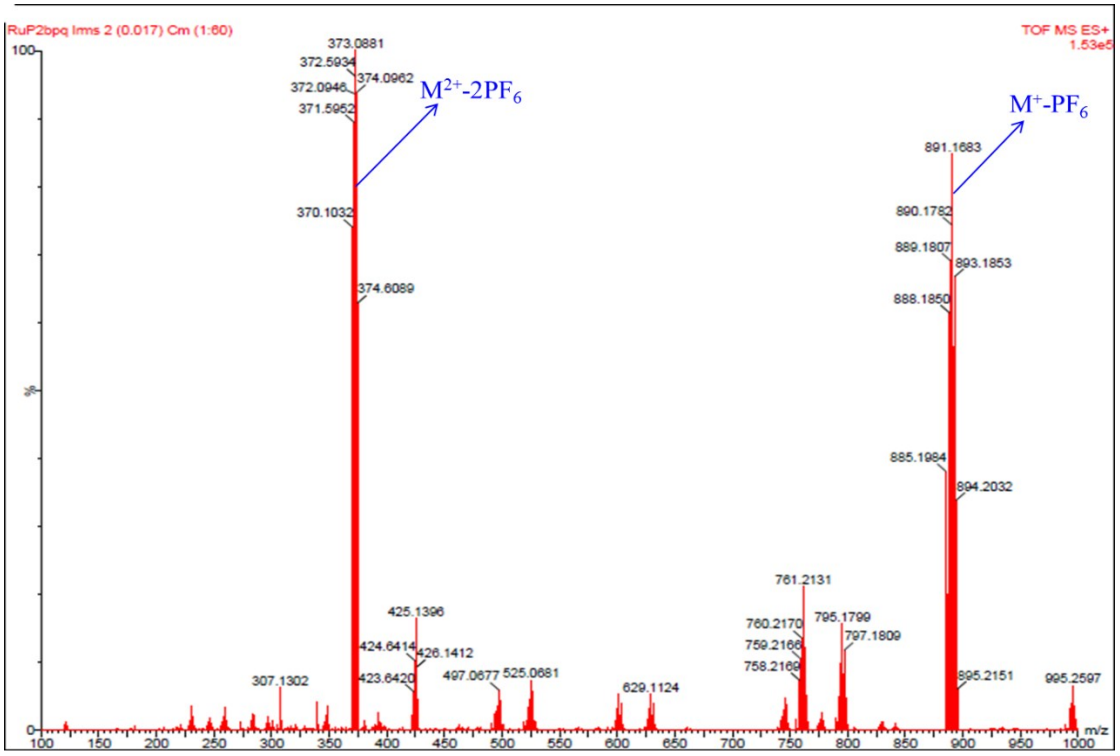

where M = $[(phen)_2Ru(bpq)](PF_6)_2$

Figure 5 TOF-MS spectra of $[(phen)_2Ru(\mu\text{-}bpq)](PF_6)_2$.

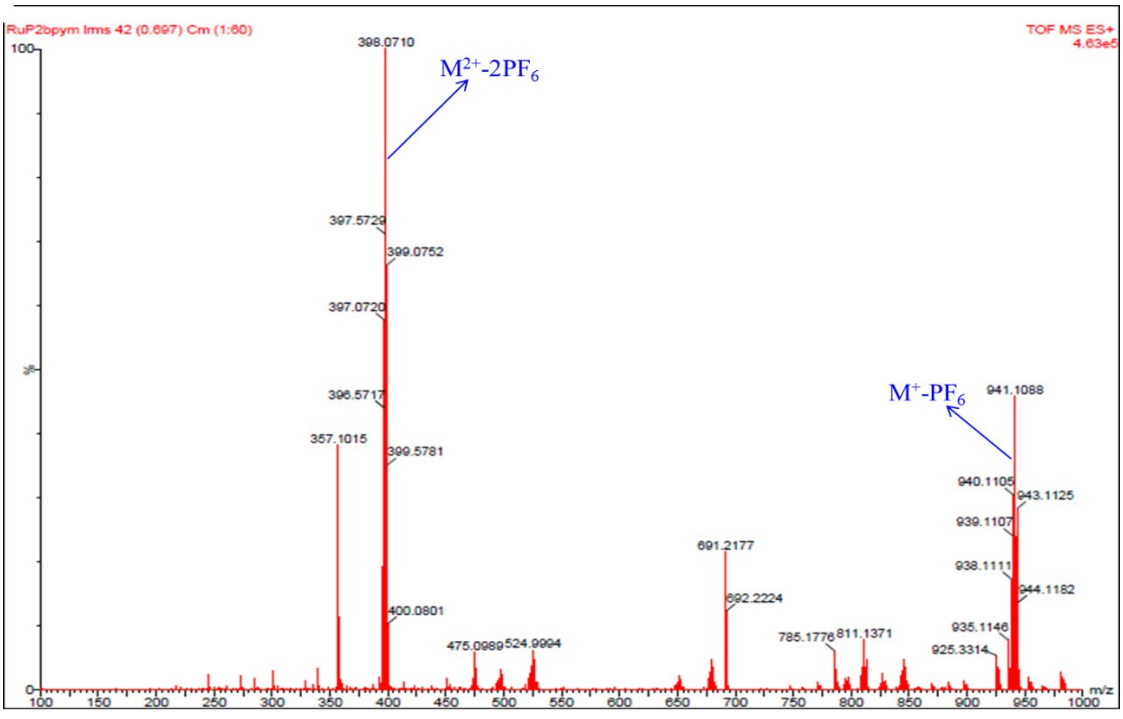

where M = $[(phen)_2Ru(bbq)](PF_6)_2$

Figure 6 TOF-MS spectra of $[(phen)_2Ru(\mu\text{-}bbq)](PF_6)_2$.

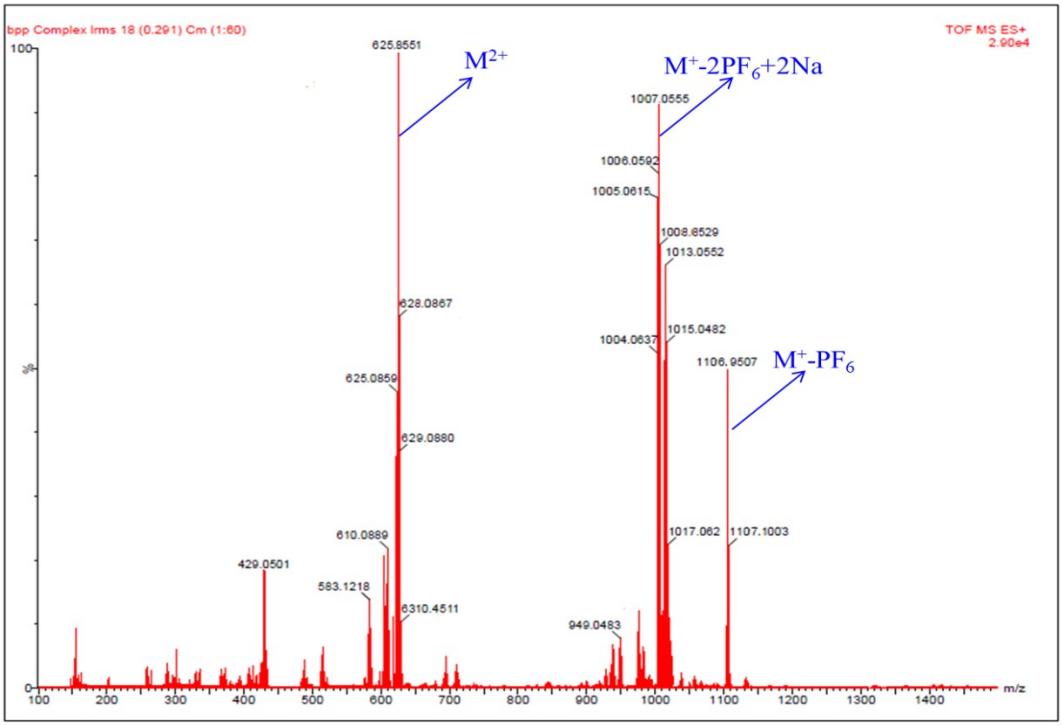

where M = $[(phen)_2Ru(bpp)PtCl_2](PF_6)_2$

Figure 7 TOF-MS spectra of $[(phen)_2Ru(\mu\text{-}bpp)PtCl_2](PF_6)_2$.

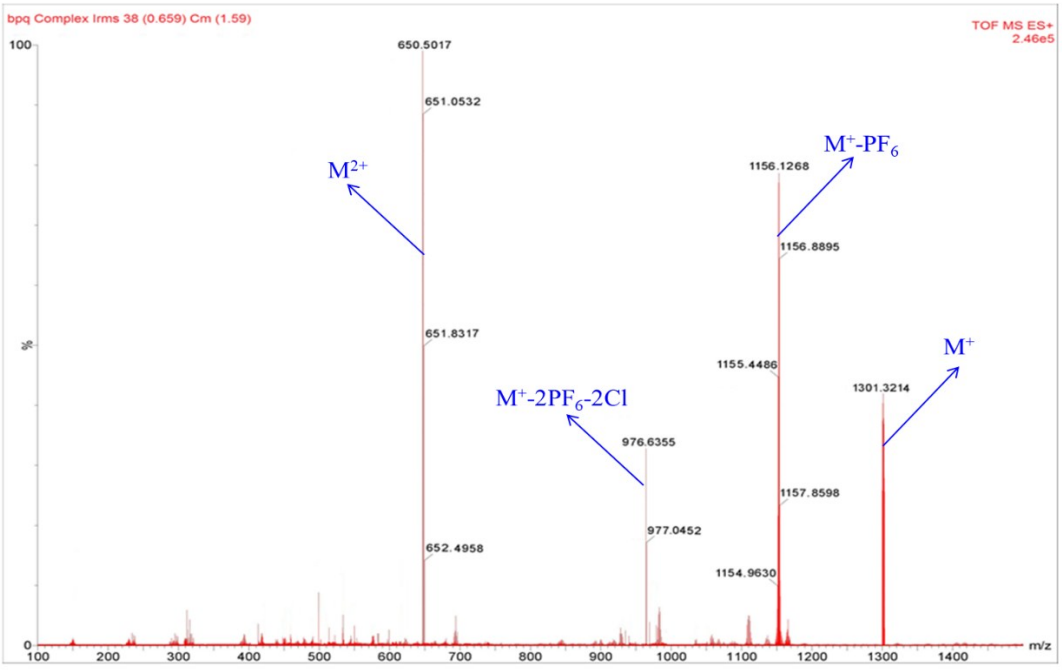

where M = $[(phen)_2Ru(bpq)PtCl_2](PF_6)_2$

Figure 8 TOF-MS spectra of $[(phen)_2Ru(\mu\text{-}bpq)PtCl_2](PF_6)_2$.

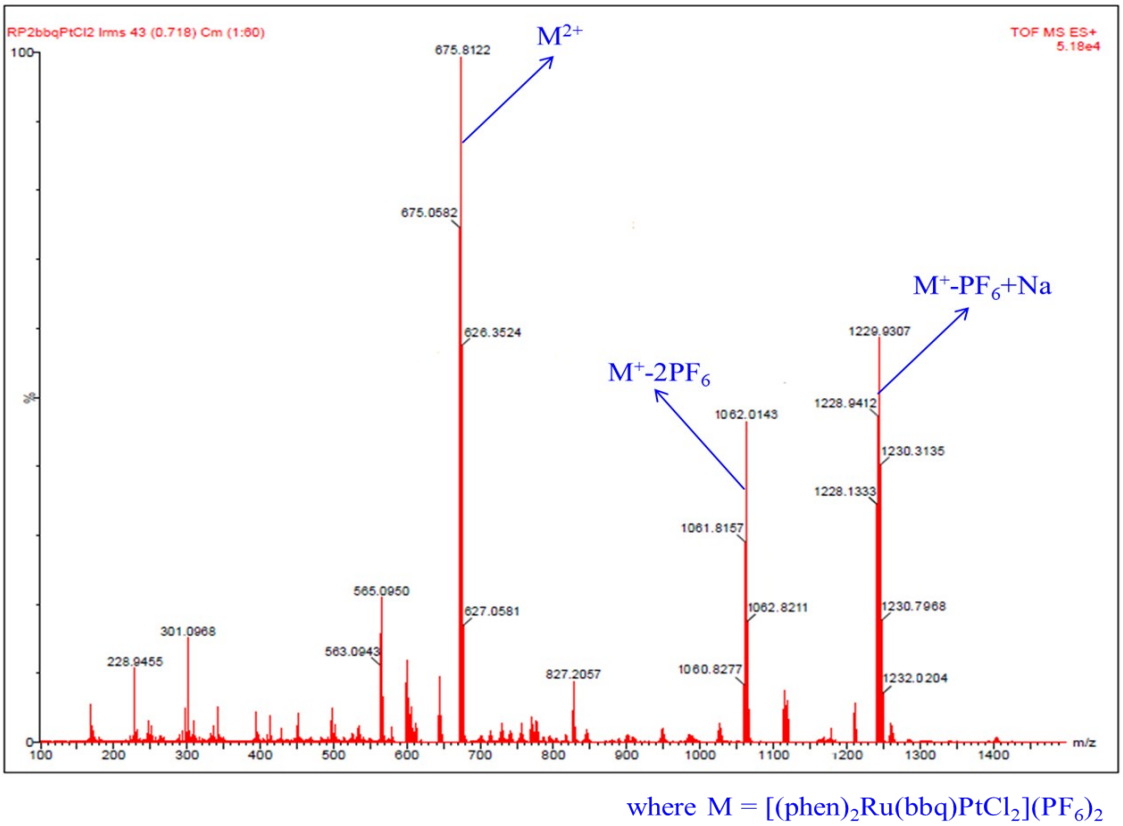

Figure 9 TOF-MS spectra of $[(phen)_2Ru(\mu\text{-}bbq)PtCl_2](PF_6)_2$.

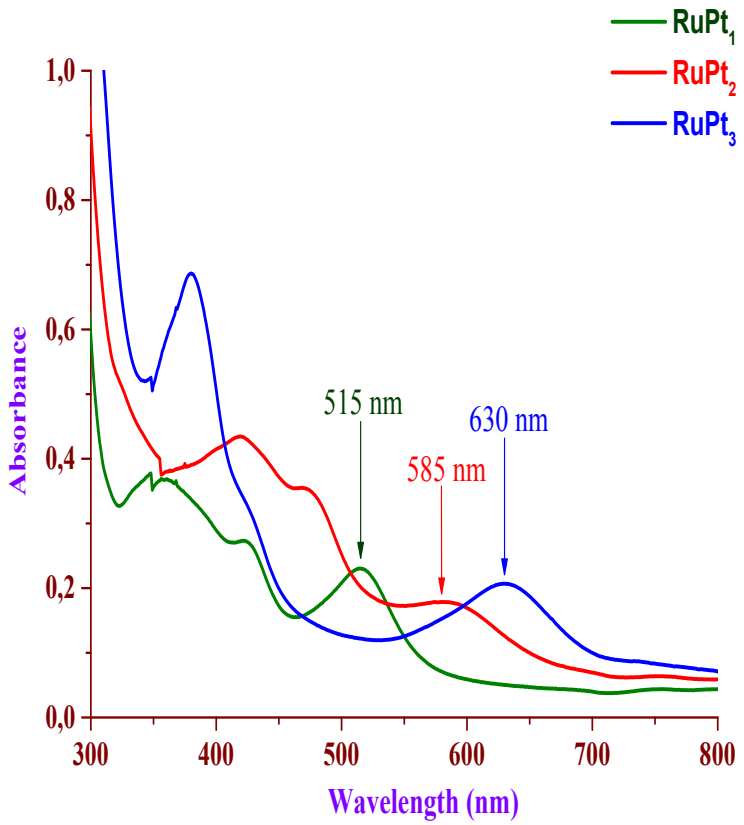

Figure 10 UV-Visible spectra of **RuPt** complexes ([RuPt] = 5 x 10^{-5} M and I = 0.1 in methanol medium)

Table 1 Summary of the second order rate constants, k_2 for the first and second steps of the title complexes with Nu at different temperatures.

Complex	Nu	k_2/M^{-1} s^{-1}					
		First step			Second step		
		25 °C	45 °C	55 °C	25 °C	45 °C	55 °C
RuPt$_1$	TU	2.19 ± 0.12	9.52 ± 0.19	17.24 ± 0.33	2.28 ± 0.15	7.02 ± 0.19	11.53 ± 0.31
	DMTU	0.58 ± 0.07	2.28 ± 0.16	4.28 ± 0.21	0.63 ± 0.09	2.24 ± 0.14	4.29 ± 0.24
	TMTU	0.02 ± 0.03	0.16 ± 0.09	0.38 ± 0.18	0.008 ± 0.05	0.08 ± 0.07	0.18 ± 0.15
RuPt$_2$	TU	90.11 ± 0.4	244.17 ± 1	385.67 ± 1	7.00 ± 0.10	32.64 ± 0.3	64.00 ± 0.3
	DMTU	66.67 ± 0.3	167.54 ± 1	262.86 ± 1	2.76 ± 0.08	9.27 ± 0.18	15.12 ± 0.27
	TMTU	9.24 ± 0.16	32.22 ± 0.3	56.23 ± 0.5	1.73 ± 0.05	4.95 ± 0.11	8.04 ± 0.16
RuPt$_3$	TU	321.05 ± 1	758.33 ± 2	1110.02 ± 3	8.83 ± 0.14	47.47 ± 0.31	96.16 ± 0.62
	DMTU	197.08 ± 1	465.09 ± 1	692.26 ± 2	3.39 ± 0.11	18.11 ± 0.20	31.69 ± 0.29
	TMTU	12.07 ± 0.22	41.05 ± 0.7	66.75 ± 0.5	1.94 ± 0.06	6.72 ± 0.16	10.76 ± 0.22

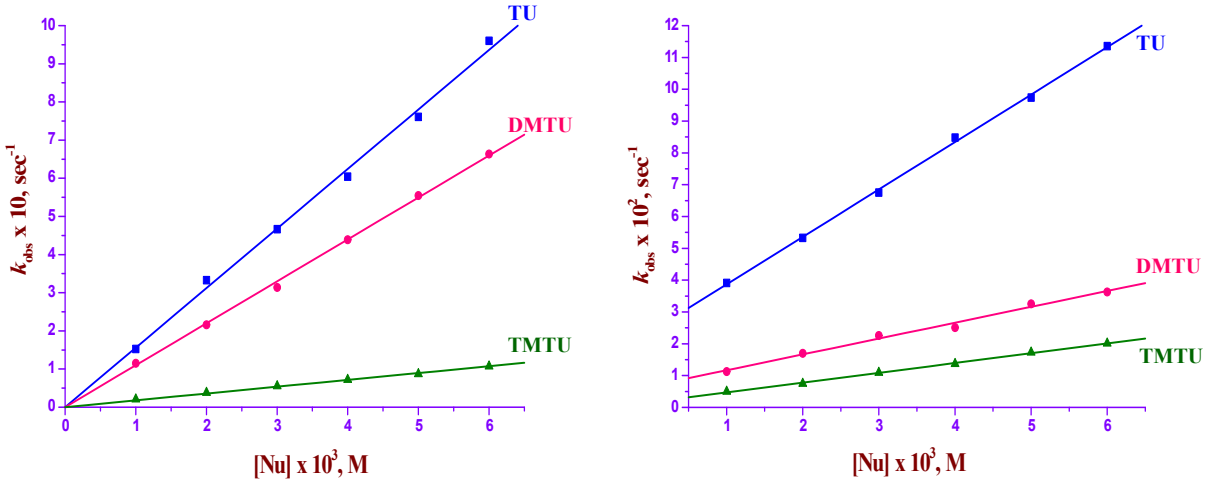

Figure 11 Dependence of the pseudo-first-order rate constants, k_{obs}^{1st} (a) and k_{obs}^{2nd} (b) on [Nu] of the reaction with **RuPt$_2$** (5 x 10^{-5} M) in methanol medium, I = 0.1 M ($NaClO_4$) at T = 35 °C

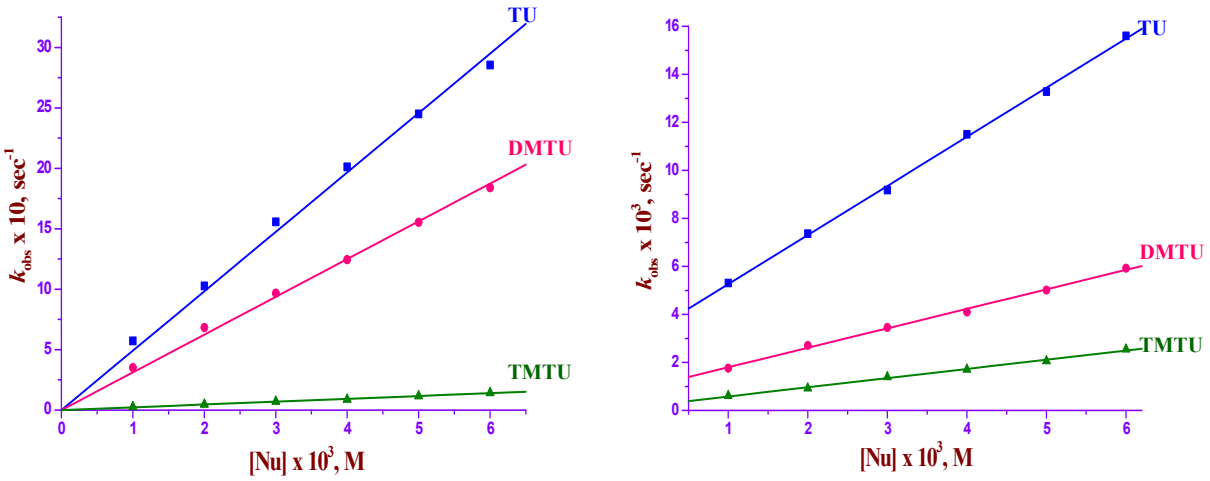

Figure 12 Dependence of the pseudo-first-order rate constants, k_{obs}^{1st} (a) and k_{obs}^{2nd} (b) on [Nu] of the reaction with **$RuPt_3$** (5 x 10^{-5} M) in methanol medium, I = 0.1 M ($NaClO_4$) at T = 35 °C

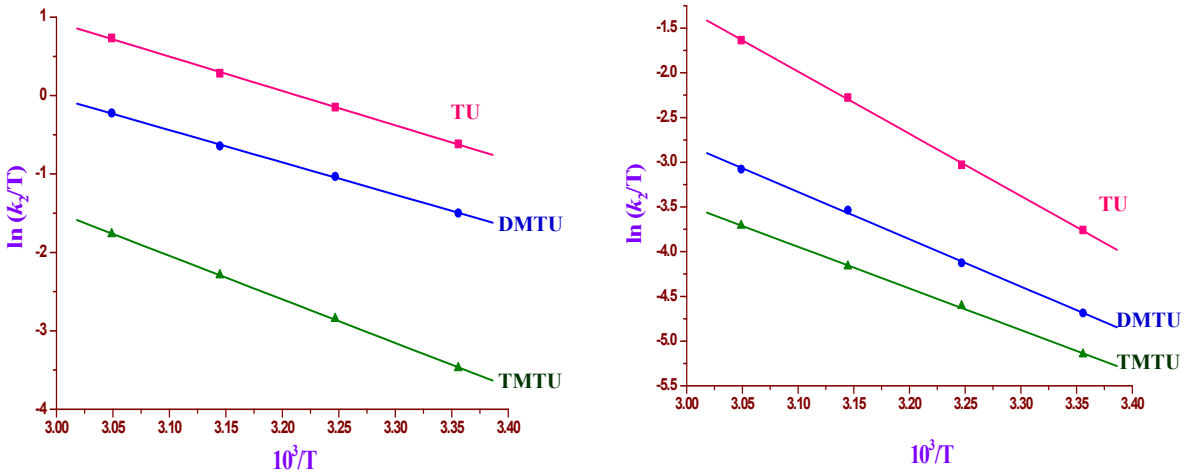

Figure 13 Eyring plots for the first (a) and second steps (b) for the substitution reaction of **$RuPt_2$** by thiourea nucleophiles.

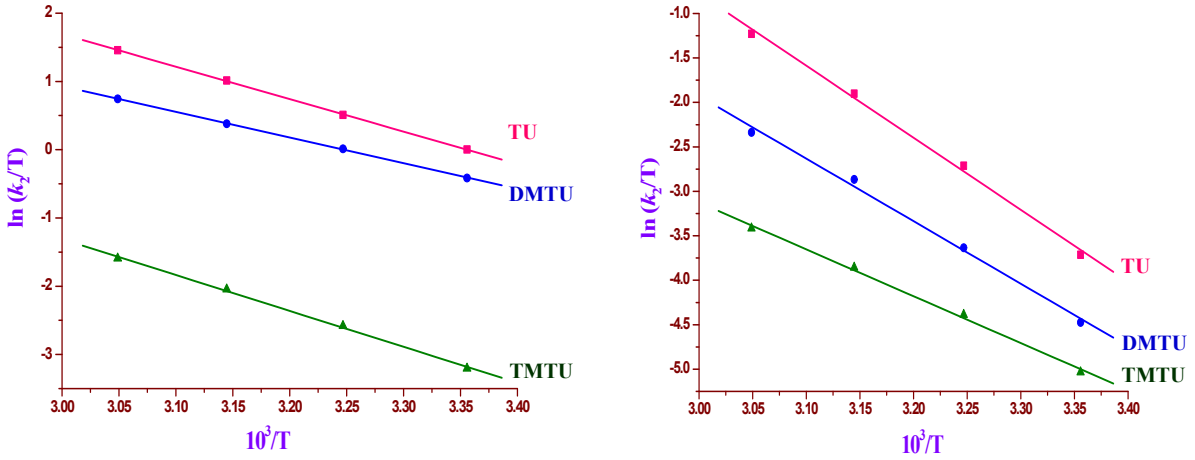

Figure 14 Eyring plots for the first (a) and second steps (b) for the substitution reaction of **$RuPt_3$** by thiourea nucleophiles.

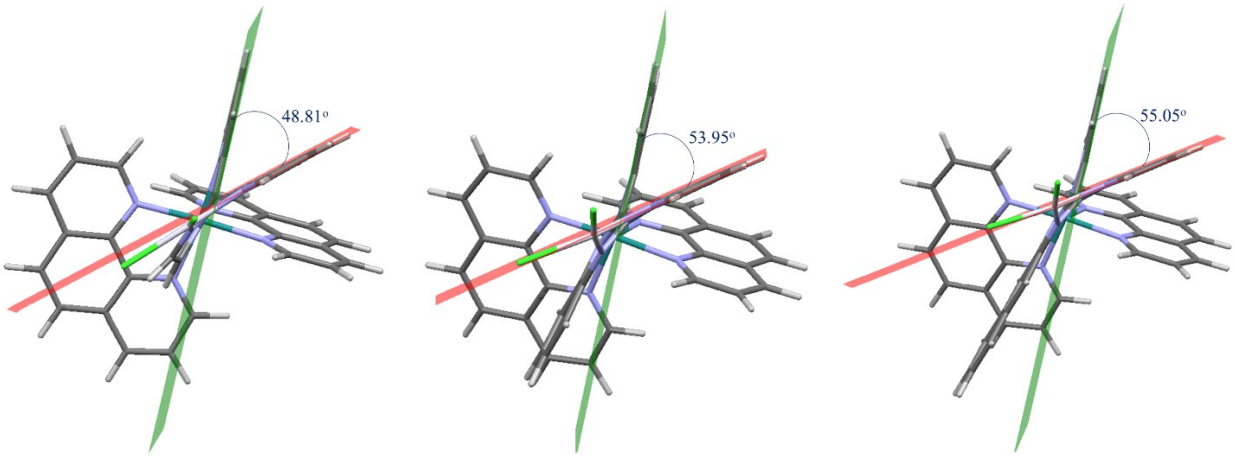

$RuPt_1$ **$RuPt_2$** **$RuPt_3$**

Figure 15 DFT-optimized structure of **RuPt** complexes showing the interplane angles between the planes passing through bridged pyridyl rings.